A Micropower Dry-Electrode ECG Preamplifier

Martin J. Burke* and Denis T. Gleeson

***Abstract*—This paper describes the development of a very low-power preamplifier intended for use in pasteless-electrode recording of the human electrocardiogram. The expected input signal range is 100 μV–10 mV from a lead-II electrode configuration. The amplifier provides a gain of 43 dB in a 3-dB bandwidth of 0.05 Hz–2 kHz with a defined high input impedance of 75 MΩ. It uses a driven common electrode to enhance rejection of common-mode interfering signals, including low-frequency motion artifact, achieving a common-mode rejection ratio (CMRR) of better than 80 dB over its entire bandwidth. The gain and phase characteristics meet the recommendations of the American Heart Association, ensuring low distortion of the output ECG signal and making it suitable for clinical monitoring. The amplifier has a power consumption of 30 μW operating from a 3.3-V battery and is intended for use in small, lightweight, portable electrocardiographic equipment and heart-rate monitoring instrumentation.**

***Index Terms*—Dry electrodes, electrocardiogram (ECG) amplifiers, ECG recording, instrumentation amplifiers, low power.**

I. Introduction

In recent years, advances in technology have brought about a considerable increase in the number of portable, battery operated, medical instruments in use in hospitals and clinics world-wide. This has been particularly true in the case of electrocardiographic equipment, which has become increasingly portable and more widespread in use on the wards as well as on out-patients. Monitoring of the ECG has also extended into other areas such as sports medicine and athletics, where it provides a reliable signal for measuring heart rate. In such equipment, size, weight, and battery power consumption are of primary importance.

In conventional recording of the ECG, a coupling gel is used with the electrodes which must also be placed correctly on the subject's body. However, in many nonclinical situations where the ECG is monitored, such as in professional athletics, trained personnel may not be available to prepare and place the electrodes. In such cases, it is more convenient to incorporate re-usable dry electrodes which do not require a coupling gel into an elasticated belt worn around the subject's chest.

The introduction of dry-electrode ECG recording more than two decades ago has led to the development of various specialized systems of electrodes, some of which have included built-in amplifiers [1]–[5]. These have been used mainly in research applications and have not become widespread in clinical electrocardiography. In recent years, however, the use of dry electrodes has become popular in many sports monitors, where the amplifier forms part of a larger custom integrated circuit. Clinical dry-electrode recording would be of benefit in applications where long-term monitoring of the ECG is required. Consequently, there is a need for a low-cost preamplifier that is suitable for dry-electrode recording of the ECG and provides a signal of adequate quality for clinical purposes. It should be compact, lightweight, and consume as little battery power as possible. The authors have designed a preamplifier that fulfills these requirements, using relatively inexpensive and commercially available components.

Manuscript received February 4, 1999; revised August 30, 1999. *Asterisk indicates corresponding author.*

*M. J. Burke is with the Department of Electronic and Electrical Engineering, University of Dublin, Trinity College, Dublin 2, Republic of Ireland (e-mail: mburke@tcd.ie).

D. T. Gleeson is with the Department of Electronic and Electrical Engineering, University of Dublin, Trinity College, Dublin 2, Republic of Ireland.

Publisher Item Identifier S 0018-9294(00)00896-X.

II. Design Requirements

In clinical diagnosis involving the ECG signal, it is of the utmost importance that the profile of the signal be as faithfully preserved as possible en route from the electrodes to the recorder output. The design of the recording amplifier plays a major role in achieving this [5]–[9]. The design requirements of an amplifier intended for use with dry electrodes are more stringent than is the case with conventional electrodes. However, with due care and attention it is possible to achieve comparable performance. The factors affecting the quality of the recorded ECG signal are the skin-electrode-amplifier interface, electrode motion artifact, electrical interference, amplifier CMRR, amplifier frequency response, semiconductor noise generated in the amplifier, and input signal level variation.

Variation in the signal level takes place primarily between individuals and can be counteracted by the use of automatic gain control. This was not included in the preamplifier in question and, hence, is not discussed further. The remaining factors are each considered in turn as follows.

A. The Skin-Electrode-Amplifier Interface

The electrodes used by the authors were composed of conductive graphite, lightly impregnated with aluminum (Respironics Inc.), were of circular shape of approximately 3 cm diameter and were mounted on an elasticated belt worn around the user's chest. The electrode impedance measured at several frequencies with moderate tension applied to the belt on dry skin is given in Table I. The impedance measured was lower when greater tension was applied to the belt or when sweat was present on the skin.

Many analyses have been carried out on the complex electrochemical interactions that take place at the skin-electrode interface, in order to develop an equivalent electrical model for this [10]–[13]. These can become quite complicated and often fail to yield conclusive values for the individual components of the model [2]. A simple but adequate model used by the au-

thors is shown in Fig. 1(a) where the principal elements are: V_{POL}, representing the dc polarization potential at the skin-electrode interface; C_C in parallel with R_C, representing the coupling impedance; and R_S, representing the minimum series contact resistance. The values of the elements in the model, particularly the coupling impedance, are considerably different for the dry-electrode scenario than for conventional electrodes. Values were determined which give closest agreement between the impedance of the model and that measured for the electrodes over the frequency range of interest, as can be seen from Table I.

The electrical properties of the model affect the signal that appears at the input of the recording amplifier, having an input resistance R_i as shown. The transfer function defining the relationship between the signal detected at the surface of the skin V_s and that appearing at the input of the amplifier V_i is given as

$$\frac{V_i(s)}{V_s(s)} = \frac{R_i}{R_i + R_s} \times \frac{\left(s + \dfrac{1}{C_c R_c}\right)}{\left(s + \dfrac{1}{C_c[R_c//(R_i + R_s)]}\right)}. \quad (1)$$

Bode approximations of the magnitude and phase responses of this function are shown plotted in Fig. 1(b) and it can be seen to contain a pole and a zero, with the pole having the higher frequency. The response of the combined network introduces a frequency-dependent attenuation and phase-shift into the signal present at the amplifier input. The high-frequency magnitude is given by $R_i/(R_i+R_s)$. The attenuation of the signal can be kept to an insignificant level of less than 1% by making $R_i > 100R_s$, which for the element values given requires $R_i > 1$ MΩ.

The maximum phase shift introduced by the network is 90° but is less than this if the pole and zero are close together. In order to avoid introducing phase distortion into the signal at the input to the amplifier, the pole should be kept at least a decade below the lowest frequency of interest in the signal. However, the values of R_c and C_c are generally not high enough to allow this. An alternative approach is to ensure that $R_i \gg R_c$. In this case, it can be seen from (1) that the pole and zero almost merge so that the network becomes in effect purely resistive with negligible attenuation and phase shift. A maximum phase shift of 1° requires $R_i > 60R_c \approx 80$ MΩ.

B. Electrode Motion Artifact

Movement of the subject, as takes place in exercise for example, induces pressure variations at the skin-electrode interface which generates artifact in the signal present at the amplifier input. This mechanism has been analyzed by Zipp and Ahrens [13], where the amplifier was dc coupled to the electrodes which were themselves modeled as purely resistive. In this case, a motion induced interfering signal appears at the amplifier input due to two factors: first, variation in the dc polarization potential ΔV_{POL} and second, variation in the electrode contact resistance ΔR_E. The component due to resistance variation is itself caused by two sources of dc current through the resistance: the input bias current of the amplifier i_B and the current flowing due to the polarization potential V_{POL}/R_i. The

TABLE I
IMPEDANCE VALUES FOR THE DRY ELECTRODES AND THE EQUIVALENT MODEL OF FIG. 1(a) AT DIFFERENT FREQUENCIES

Frequency:	0.1	1.0	10	50	100	1000	Hz.
Electrode Impedance:	1360	1360	416	152	101	17	kΩ
Model Impedance:	1360	1200	508	152	85	17	kΩ

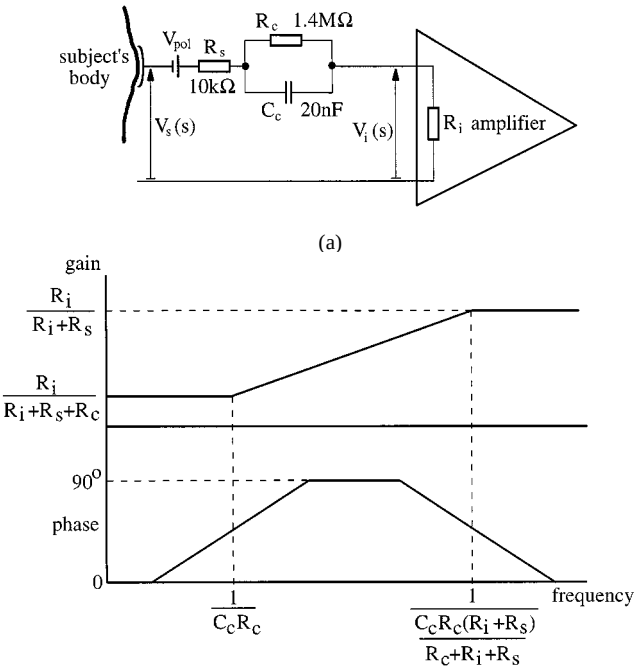

Fig. 1. A model of the skin-electrode-amplifier interface: (a) equivalent electrical circuit and (b) Bode approximations of the gain and phase responses.

motion artifact signal appearing at the amplifier input V_{mot} is then given as

$$V_{mot} = \Delta V_{POL} + \Delta R_E \left(i_B + \frac{V_{POL}}{R_i}\right). \quad (2)$$

Zipp and Ahrens deduced that in order to keep the resistive interfering component to less than 10 μV, with both currents contributing equally to it, $i_B < 50$ pA and $R_i > 1$ GΩ. However, if ac rather than dc coupling is employed, then dc current does not flow through the electrodes and the resistive component of the motion artifact due to this effect is eliminated. In this case, the amplifier input impedance does not need to be as high as 1 GΩ and its magnitude requirement is governed by the factors discussed in Section II-A.

In addition, the use of ac coupling also allows a higher gain to be implemented in the first stage of the amplifier than is the case with dc coupling as the dc polarization voltage is blocked from the amplifier input. Very low frequency drift in the polarization potential will be also be attenuated. The ac coupling will

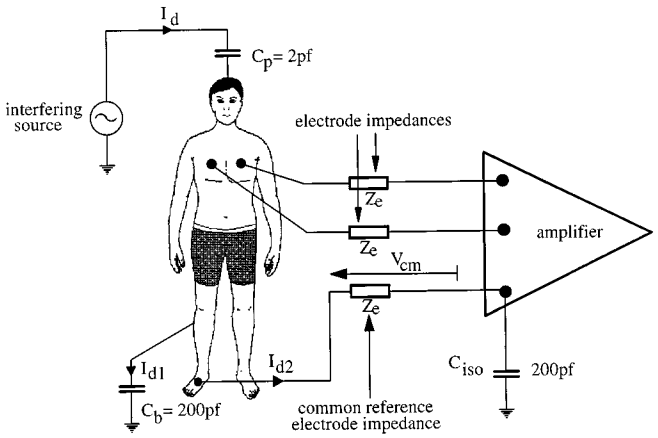

Fig. 2. Electrostatic interference.

not, however, eliminate in-band interference due to direct variation in the potential caused by movement of the electrodes or noise induced by the presence of sweat. These effects cannot be counteracted by design of the amplifier input stage.

C. Electrical Interference

Unwanted signals can also be superimposed on the wanted ECG signal at the amplifier input by means of electrical interference. Some of this interference can be filtered out as it is out-of-band, but the largest portion is often in-band, particularly that caused by the mains power supply. Mains hum can be introduced into the ECG by two means, namely electromagnetic induction and electrostatic induction [14], [15]. In the case of electromagnetic induction, the magnetic field associated with the mains supply current flowing in nearby electrical equipment cuts the loop enclosed by the subject, the electrode leads and the amplifier and induces an electromotive force (emf) in the leads. This emf is directly proportional to the area of the loop but can be rendered negligible by twisting the leads together to minimize this area [14]. With the electrodes and a preamplifier mounted on a belt worn around the subject's chest, there is little or no loop area involved and hence this type of interference is not prevalent.

In the case of electrostatic induction, the electric field associated with the mains supply is capacitively coupled to the subject who is also coupled to ground via the body capacitance C_B as shown in Fig. 2. This is of particular importance in battery-operated instruments when the common supply line of the amplifier is not at true earth potential and there is also an isolation capacitance C_{iso} present [15]. A displacement current I_d then flows through the subject to ground, splitting between the two paths as shown. This current develops an interfering signal at each of the electrodes relative to ground and consequently at the input to the recording amplifier. When the electrodes are mounted close together on the subject, or are symmetrically placed on the body relative to ground, the differential component of this interfering signal is minimal and it becomes predominantly common-mode. It has been found that the body and isolation capacitances have similar magnitudes [15], [16] and at mains supply frequency these have a reactance of the order of 15 MΩ, which is much greater than the body and electrode impedances. Hence, the common-mode potential at either electrode with respect to the amplifier common can be estimated as $V_{cm} = (i_d/2)Z_e$. Displacement currents of the order of 0.5 μA have been measured by the authors, which agree with figures previously reported in the literature [14], [17]. This gives a common-mode interfering signal level of 37.5 mV. The CMRR of the amplifier must then be relied upon to suppress this interference. The minimum input ECG signal level to the amplifier is intended to be 100 μV. If the error at the amplifier output due to the common-mode input signal is to be kept to a maximum of 5%, then a CMRR of 77 dB is required.

D. Amplifier Common-Mode Rejection Ratio

The schematic diagram of a standard instrumentation amplifier is shown in Fig. 3. The majority of ECG amplifier input-stages can be shown to have an equivalent structure of this form. The electrode impedance is $Z_E \pm \Delta_E Z_E$, the common-mode impedance measured from each amplifier input terminal to ground is $Z_C \pm \Delta_C Z_C$ and the differential impedance measured between the input terminals is Z_d. There are three primary factors which limit the CMRR obtainable, namely: common-mode impedance mismatch at the amplifier input, manufacturing tolerances in the gain-determining resistors, and the finite CMRR's of the op-amps used to implement the amplifier [14]–[21].

A common-mode signal present at the input to the electrodes gives rise to a differential component at the amplifier input, due to mismatch in the common-mode impedances on either side of the amplifier. Once present here, this component receives the same gain as the differential input signal. The CMRR due to the impedance mismatch can be taken as the ratio of this differential component to the input common-mode component causing it and is given for worst case mismatch as [18], [19]

$$\mathrm{CMRR}_{\Delta Z} = 20\log_{10}\left[\frac{Z_C}{Z_E}\right] + 20\log_{10}\left[\frac{1-\Delta_C^2}{2(\Delta_C+\Delta_E}\right] \text{ dB}. \quad (3)$$

It should be noted that this depends on the magnitude of Z_C in relation to Z_E as well as the degree of variation in these impedances. With $Z_C = 60Z_E$ to meet the requirements imposed by the skin-electrode interface considered previously and $\Delta Z_E = \Delta Z_C = 10\%$, then $\mathrm{CMRR}_{\Delta Z} \approx 44$ dB. This is well below the value required to adequately suppress common-mode interference.

The CMRR due to a manufacturing tolerance, $\pm\Delta_R$ in the gain-determining resistors, when these are assigned to give the highest degree of imbalance between the inverting and noninverting sides of the amplifier, can be shown to be [18], [20], [21]

$$\mathrm{CMRR}_{\Delta R} = 20\log_{10}\left(1+2\frac{R_2}{R_1}\right)\left(\frac{1+\dfrac{R_4}{R_3}}{4\Delta_R}\right) \text{ dB}. \quad (4)$$

This shows that the effect of the resistor mismatch in the differential-to-single-ended second stage of the amplifier is reduced by the gain of the preceding differential input stage. It is also the case that the mismatch of the resistors in the differential stage

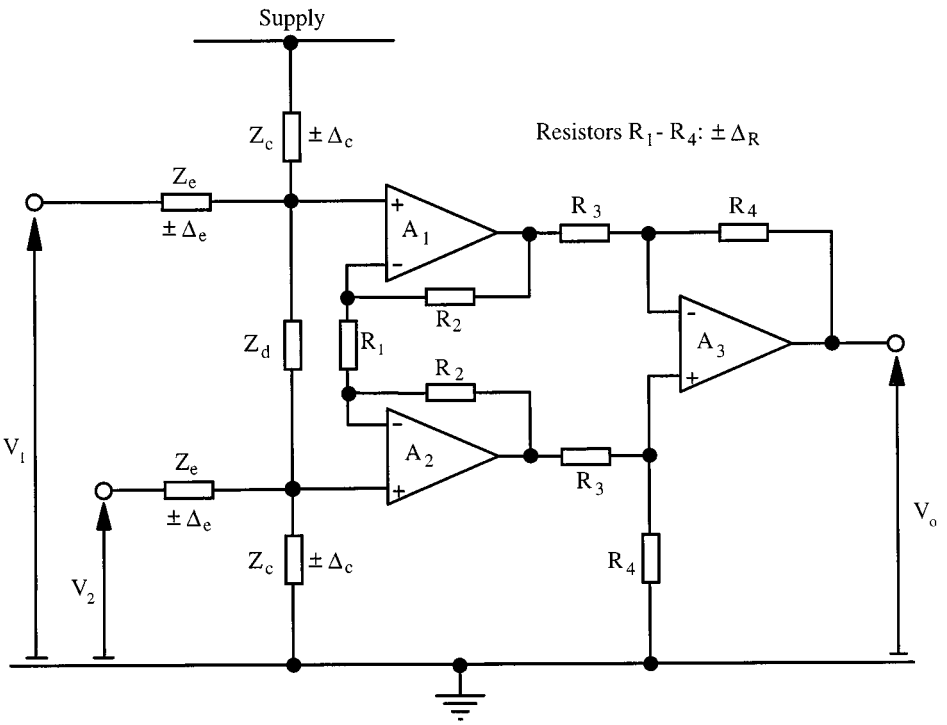

Fig. 3. A standard instrumentation amplifier.

does not influence the CMRR because of the cross-symmetrical nature of this stage. This favors the use of as high a gain as possible in both stages of the amplifier as well as the use of low-tolerance resistors.

The final component of the overall CMRR is determined by the CMRR's of the individual op-amps used to implement the amplifier. This is given as [18], [20], [21]

$$\frac{1}{\mathrm{CMRR}_{op}} = \frac{1}{\mathrm{CMRR}_{op1}} + \frac{1}{\mathrm{CMRR}_{op2}} + \frac{1}{\left(1+2\dfrac{R_2}{R_1}\right)(\mathrm{CMRR}_{op3})}. \quad (5)$$

It can be seen that the CMRR of the op-amp used in the differential-to-single-ended stage is less significant than that of the other op-amps by a factor equal to the gain of the differential-input stage. If the latter is high and if all op-amps are identical, then $\mathrm{CMRR}_{op} = 1/2(\mathrm{CMRR}_{op1})$, or 6 dB lower than that of a single op-amp.

The overall CMRR of the amplifier is determined by the combined effects of each of the contributing components as

$$\frac{1}{\mathrm{CMRR}} = \frac{1}{\mathrm{CMRR}_{\Delta Z}} + \frac{1}{\mathrm{CMRR}_{\Delta R}} + \frac{1}{\mathrm{CMRR}_{op}}. \quad (6)$$

In general, one of these individual factors usually predominates in determining the overall CMRR. If the CMRR of the op-amps and the gain of the front-end stages of the amplifier are reasonably high, the impedance conditions at the amplifier input become the limiting factor.

E. Amplifier Frequency Response

If the ECG signal profile is to be preserved without distortion, then the amplifier must have the appropriate gain and phase versus frequency characteristics. The gain must be constant within the frequency range of the signal and a sufficiently linear phase characteristic must prevail over the same range. The American Heart Association [22], [23] recommends that ECG recorders should have a 3 dB frequency range extending from 0.67 Hz to 150 Hz. The magnitude of the response should be flat to within ± 0.5 dB within the range of 1Hz to 30 Hz. The phase shift introduced at the low end of the spectrum should not exceed that of a first-order high-pass network with a pole at 0.05 Hz.

F. Semiconductor Noise

In its passage through the amplifier, the signal quality is degraded slightly by added noise. The equivalent circuit of a noninverting op-amp structure that can be used for noise analysis is shown in Fig. 4(a). The total rms output noise voltage of this structure is given by (7), shown at the bottom of the page, where

v_{na} noise voltage of the op-amp, referred to its input;
i_{na} noise current of the op-amp, referred to its input;

$$v_{no} = \sqrt{\left(1+\frac{R_2}{R_1}\right)^2 v_{na}^2 + i_{na}^2 R_2^2 + \left(1+\frac{R_2}{R_1}\right)^2 i_{na}^2 R_i^2 + \left(1+\frac{R_2}{R_1}\right)^2 v_{nR_i}^2} \quad (7)$$

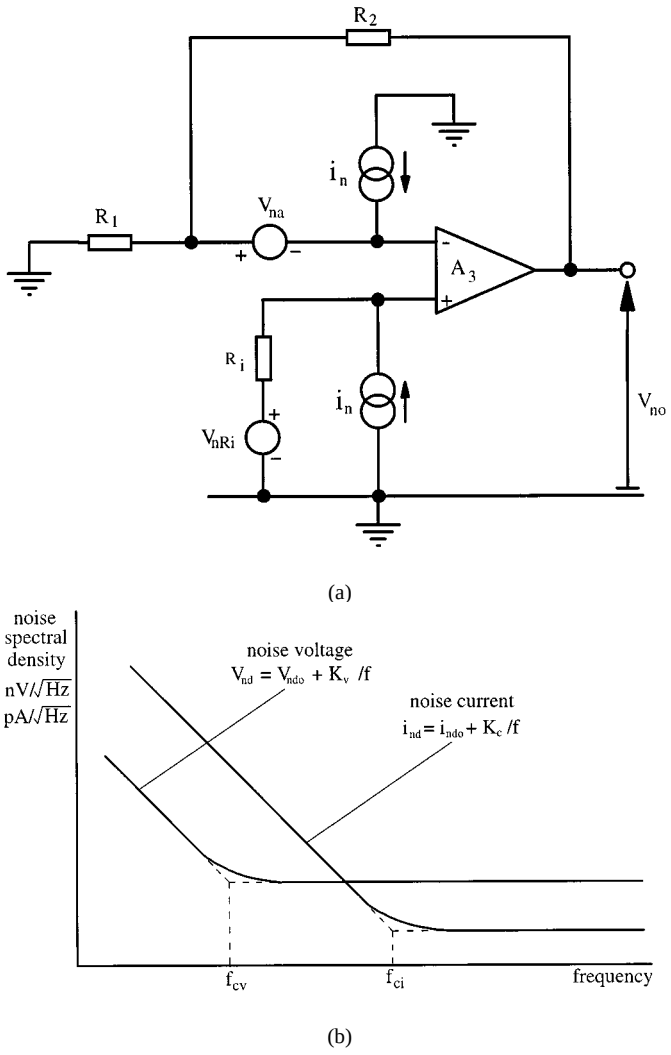

Fig. 4. Operational amplifier noise characteristics: (a) equivalent noise model for a noninverting amplifier and (b) a plot of typical op-amp noise voltage and current spectral densities.

v_{nR_i} noise voltage generated by the equivalent input resistance, R_i.

The noise generated by the resistors R_1 and R_2 is considered negligible compared to that of the other sources. The output noise voltage can be scaled by a factor of $\sqrt{2}$ when considering a differential instrumentation amplifier input stage.

The profiles of the noise voltage and noise current as functions of frequency are shown for a typical operational amplifier in Fig. 4(b). It can be seen that both profiles show a predominantly white noise character at medium and high frequencies and a $1/f$ or flicker type character at frequencies below a corner frequency. The corner frequencies, f_{cv} and f_{ci}, usually lie within the ECG signal spectrum and a knowledge of these is required as well as the white noise values, v_{ndo} and i_{ndo}, to allow an accurate estimation of the output noise voltage. Integrating these profiles over the frequency range from f_L to f_H gives [19]

$$v_{na}^2 = v_{ndo}^2 \left[(f_H - f_L) + 2f_{cv} \ln \left(\frac{f_H}{f_L} \right) + f_{cv}^2 \left(\frac{f_H - f_L}{f_H f_L} \right) \right] \quad (8)$$

and

$$i_{na}^2 = i_{ndo}^2 \left[(f_H - f_L) + 2f_{ci} \ln \left(\frac{f_H}{f_L} \right) + f_{ci}^2 \left(\frac{f_H - f_L}{f_H f_L} \right) \right]. \quad (9)$$

These expressions can be evaluated and the results substituted into (7) to determine the output noise voltage, which can then be referred to the amplifier input by dividing by the gain. If the rms noise level is to remain at least 20 dB below the minimum signal level of 100 μV, then the input referred noise voltage must be less than 10 μV rms. If the noise were truly Gaussian in character, the probability of the peak-to-peak voltage exceeding 3.3 times the rms value would be less than 0.1%. Consequently, a reasonable limit on the peak-to-peak input-referred noise voltage is 25–30 μV.

III. Circuit Outline

A schematic diagram of the preamplifier designed by the authors, which is intended to meet the above requirements is shown in Fig. 5. It is a very low-power circuit operating from a 3.3 V supply and is intended for use in dry-electrode recording of the ECG under exercise conditions. The specified input signal level ranges from 100 μV to 10 mV. The amplifier consists of two differential-input-differential-output stages followed by a differential-to-single-ended stage. The operational amplifiers used were selected from the MAX400 series (Maxim Inc.). This series was chosen for its extremely low power consumption, the quiescent current being typically 1 µA per op-amp. Op-amps A_1, A_2, A_5, and A_6 are of the type MAX406A, chosen for its low input offset voltage of 0.5 mV, while A_3 and A_4 are of the type MAX419 which has a larger gain-bandwidth product of 80 kHz.

The front-end differential stage of the amplifier is ac coupled via capacitors C_1 and C_2, which are chosen to provide a low-frequency response which does not cause phase distortion of the ECG signal. Resistors R_1 and R_2 are current-limiting, protection resistors which prevent transient current spikes from reaching the subject, but are of negligible magnitude compared to the electrode impedances. The dc bias voltages, required for single-supply operation, are provided by resistors R_5, R_6, and R_7 and are chosen to ensure that common-mode input voltages to the op-amps are kept at least 1.2 V away from either supply rail. The bias voltages are fed to both inverting and noninverting sides of the op-amps A_1 and A_2 so that the output dc voltages are the same as those at the input of each op-amp. The resistors R_3 and R_4 are used to define the input impedance on each side of the amplifier. The return ends of these resistors are connected to either side of resistor R_6 which receives feedback from the outputs of op-amps A_1 and A_2 via resistors R_8, R_9, R_{10}, and R_{11}. This feedback maintains the voltages at the upper and lower ends of R_6 close to the input voltages V_1 and V_2, respectively. The potential drops across R_3 and R_4, therefore, become very small, making the magnitude of these resistors appear much higher at the amplifier inputs. This allows the

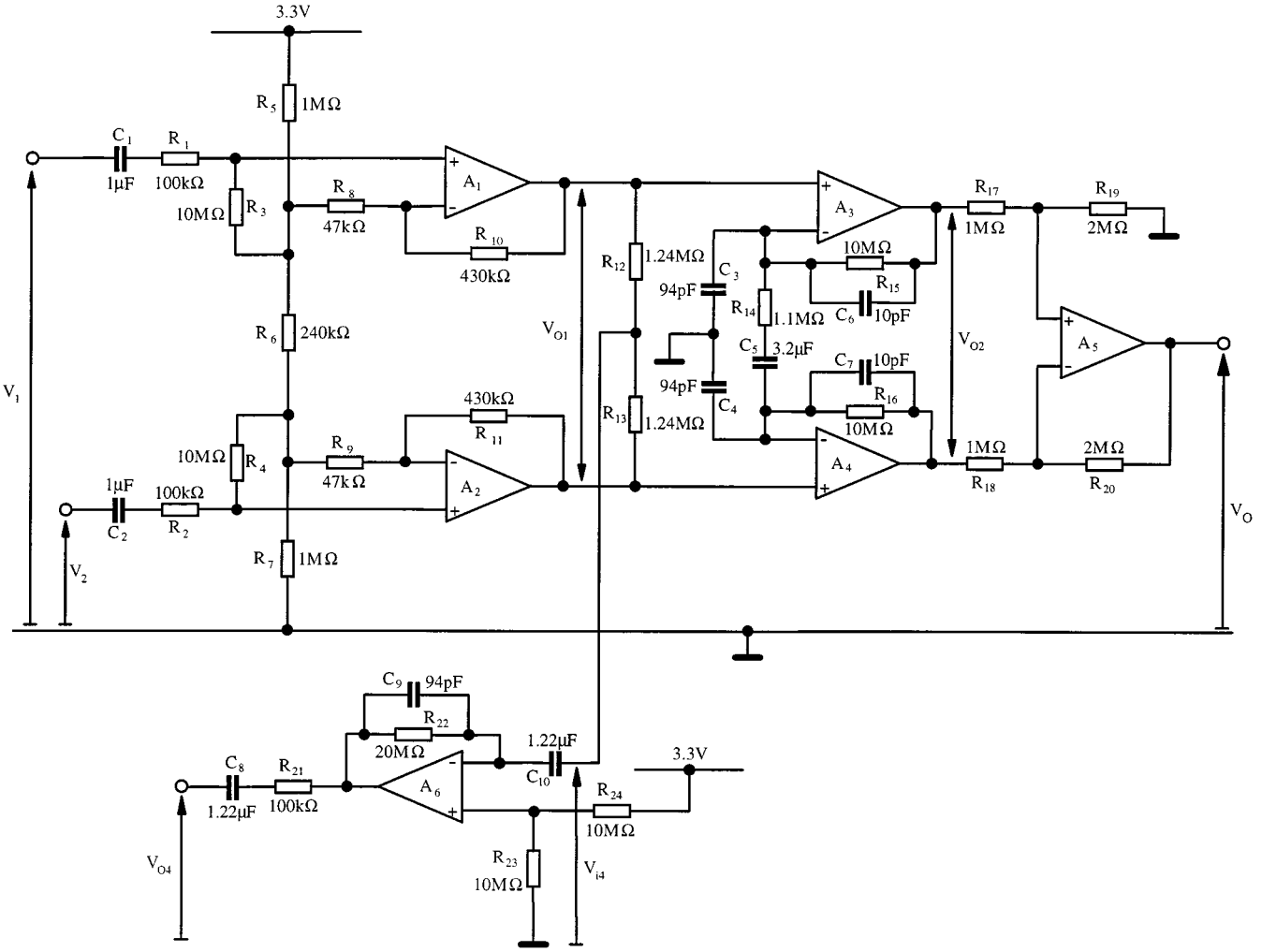

Fig. 5. Schematic diagram of the preamplifier.

requirement of a very high input impedance to be met without the use of unduly large values of resistors. The transfer function of this stage for a differential input signal, $V_{id} = V_2 - V_1$ is given as

$$\frac{V_{o1}(s)}{V_{id}(s)} = \left[1 + \frac{R_{10}}{R_8 + \left(\frac{R_5 R_6}{2R_5 + R_6}\right)}\right] \cdot \left[\frac{sC_1\left(\frac{R_c R_d}{2R_c + R_d}\right)}{1 + sC_1\left(\frac{R_c R_d}{2R_c + R_d}\right)}\right] \tag{10}$$

where R_c and R_d are the common-mode and differential input impedances, respectively, given by

$$R_c = R_3\left[\frac{R_8 + \frac{R_5(R_6+R_8)}{R_5+R_6+R_8}}{R_8}\right] \cdot \left[1 + \frac{R_5}{R_6+R_8}\right] \approx 260\ \text{M}\Omega \tag{11}$$

and

$$R_d = R_3\left[\frac{R_8 + \frac{R_5(R_6+R_8)}{R_5+R_6+R_8}}{R_8}\right] \cdot \left[1 + \frac{R_6+R_8}{R_5}\right] \approx 75\ \text{M}\Omega. \tag{12}$$

The mid-band gain of the stage is given by the first term in (10) and has a magnitude of 13 dB. The second term describes the frequency dependence of this stage and the value of C_1 is chosen to give a pole at a frequency of 0.002 Hz, which counteracts the effect of a zero in the transfer function of the following stage. The only drawback of this stage is the fact that the input offset voltages of the op-amps appear augmented at their outputs by a factor which is much higher than the mid-band gain of the stage. If the input offset voltages of op-amps A_1 and A_2 are of equal magnitude and opposite polarity $\pm V_{osi}$, it can be shown

that the magnitude of the output offset voltage of each op-amp is quantified as [21]

$$V_{oso} = \frac{R_{10} + \left(\frac{R_5 R_6}{R_5 + R_6}\right)}{R_8} . V_{osi}. \tag{13}$$

Consequently, the op-amps used as A_1 and A_2 must have low-input offset voltages and the gain of this stage must be kept to a modest value.

The second stage of the amplifier is also a differential-input stage. This stage is dc coupled at the input, but the resistor-capacitor combination R_{14} and C_5 limits the dc gain to unity. The appropriate choice of component values allows the combined low-frequency response of the first and second stages to be that of a single pole at 0.05 Hz, thus avoiding phase distortion of the signal. The differential gain of the second stage is given as

$$\frac{V_{o2}(s)}{V_{o1}(s)} = 1 + \frac{2sC_5R_{15}(1 + s\frac{1}{2}C_3R_{14})}{(1 + sC_6R_{15})(1 + sC_5R_{14})}. \tag{14}$$

It was discovered during the design process that the input capacitances of the op-amps A_3 and A_4 introduce a zero into the high frequency response of this stage, giving rise to instability. In order to overcome this, capacitors C_3 and C_4 were added at the op-amp inputs to define the zero more reliably. The capacitors C_6 and C_7 are, therefore, included across resistors R_{15} and R_{16} to introduce a pole which cancels this zero by making $2C_6R_{15} = 2C_7R_{16} = C_3R_{14} = C_4R_{14}$. This makes the high-frequency response of the second stage stable again, being then limited by the open-loop gain of the op-amps. The mid-band gain of this stage is $1 + 2(R_{15}/R_{14}) = 25.6$ dB.

The final output stage of the amplifier is a differential-to-single-ended stage which is dc coupled, with only resistive components used in conjunction with op-amp A_5. This allows better matching of component values which preserves the CMRR of this stage at very low frequencies, thus helping to suppress interfering signals in the range just above 0.05 Hz within the passband of the amplifier. Because of the dc coupling, the gain of this stage is low and is given by $R_{19}/R_{17} = 6$ dB.

The overall CMRR of the amplifier is increased by the use of a driven common electrode, previously suggested by Winter and Webster [16]. Resistors R_{12} and R_{13} sense the common-mode output signal from the first stage of the amplifier. This is then inverted and amplified in the stage built around op-amp, A_6 and is then fed back to the common electrode via resistor R_{21} and capacitor C_8. This signal is, therefore, effectively subtracted from the common-mode interfering signal present at the amplifier inputs. This has the effect of increasing the rejection of common mode input signals by a factor equal to the gain of the inverting stage. The transfer function of this stage is given as

$$\frac{V_{o4}(s)}{V_{i4}(s)} = -\frac{\frac{s}{\left(\frac{1}{2}C_9R_{12}\right)}}{(s + 1/C_9R_{22})(s + 1/\frac{1}{2}C_{10}R_{12})} \tag{15}$$

with a mid-band value of 30 dB. The lower cutoff frequency was 0.2 Hz while the higher cutoff frequency was limited to 85 Hz to maintain stability.

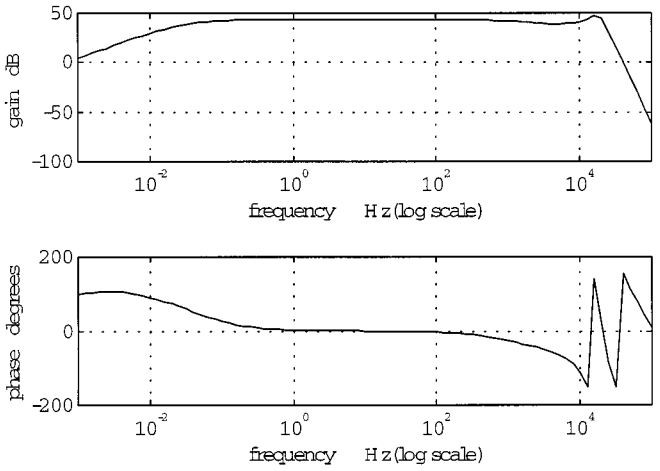

Fig. 6. A plot of the preamplifier frequency response.

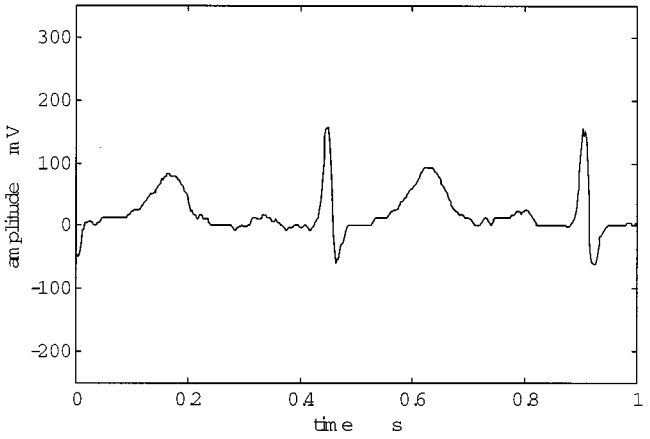

Fig. 7. An ECG recording obtained from an exercising subject.

IV. Performance Evaluation

Simulations of the circuit were carried out using PSpice during design of the amplifier. Following construction of a prototype, bench tests were carried out which gave results that were in close agreement with those of the simulations. A plot of the gain and phase versus frequency characteristics is shown in Fig. 6. The 3-dB bandwidth of the amplifier extends from 0.048 Hz to 1.9 kHz, with a mid-band gain of 43 dB. The phase at 0.5 Hz is 5.4° while that at 200 Hz is −5.8°. The high-frequency response of the amplifier is limited by the properties of the op-amps and any further bandlimiting is intended to be implemented in a subsequent amplifier. The slight peak in the magnitude response at high frequencies appearing in the simulation was not present in the prototype amplifier.

The loop gain and phase responses versus frequency of the feedback loop driving the common electrode were also measured. The 3-dB bandwidth of this loop extended from 0.2 Hz to 79 Hz, with a mid-band loop gain of 33 dB. The phase margin of the loop was measured as 74° at a frequency of 3.16 kHz, while the gain margin was 8.5 dB at a frequency of 12.5 kHz.

The CMRR of the amplifier was measured at greater than 55 dB throughout its bandwidth, without the driven common

electrode. This improves to 88 dB when the driven common electrode is used.

The peak-to-peak noise voltage measured at the amplifier output with the input terminals connected to the supply common was 7 mV, which when referred to the amplifier input is approximately 50 μV.

The quiescent current drawn by the amplifier from a 3.3 V supply is close to 9 μA, which gives a power consumption of 30 μW.

Finally, the recording of a lead II-ECG signal obtained from an exercising subject undergoing the Harvard step-test [24] is shown in Fig. 7. The subject's heart rate was 120 beats/min during the recording. It should be pointed out that substantial quantization noise has been added to this recording by the equipment used to obtain the graphical output.

V. Conclusion

The preamplifier presented meets the requirements of the American Heart Association for electrocardiographic equipment and provides an output signal considered acceptable for clinical use. It has been designed with the properties of the particular dry electrodes used by the authors in mind but should perform satisfactorily with any dry electrodes having similar properties and a contact impedance of 1.5 MΩ or less. The input stage may also be adapted to suit other electrodes.

The prototype amplifier was constructed on matrix board along with other circuitry but can readily be miniaturized and made self-contained using surface mounted components. With its extremely low power consumption, it can be energized from a small button cell battery so that the entire amplifier may be mounted on the elasticated belt worn by the user. This makes it ideally suitable for use with portable electrocardiographic equipment and heart rate monitoring instrumentation.

References

[1] W. H. Ko, M. R. Neuman, R. N. Wolfson, and E. T. Yon, "Insulated active electrodes," *IEEE Trans. Ind. Elect. Contr. Instrum.*, vol. IECI-17, pp. 195–198, 1970.

[2] G. E. Bergey, R. D. Squires, and W. C. Sipple, "Electrocardiogram recording with pasteless electrodes," *IEEE Trans. Biomed. Eng.*, vol. BME-18, pp. 206–211, May 1971.

[3] R. M. David and W. M. Portnoy, "Insulated electrocardiogram electrodes," *Med Biol. Eng.*, vol. 10, pp. 742–751, 1972.

[4] C. Gondron, E. Siebert, P. Fabry, E. Novakov, and P. Y. Gumery, "Non-polarisable dry electrode based on NASICON ceramic," *Med. Biol. Eng. Comput.*, vol. 33, pp. 452–457, 1995.

[5] W. H. Ko and J. Hynecek, "Dry electrodes and electrode amplifiers," in *Biomedical Electrode Technology*, A. C. Miller and D. C. Harrison, Eds. London, U.K.: Academic, 1974, pp. 169–181.

[6] A. S. Berson and H. V. Pipberger, "The low frequency response of electrocardiographs: A frequent source of recording errors," *Amer. Heart J.*, vol. 71, pp. 779–789, 1966.

[7] ——, "Electrocardiograph distortions caused by inadequate high-frequecy response of direct-writing electrocardiographs," *Amer. Heart J.*, vol. 74, pp. 208–219, 1967.

[8] D. Tayler and R. Vincent, "Signal distortion in the electrocardiogram due to inadequate phase response," *IEEE Trans. Biomed. Eng.*, vol. BME-30, pp. 352–356, June 1983.

[9] M. P. Watts and D. B. Shoat, "Trends in electrocardiograph design," *J. Inst. Electron. Rad. Eng.*, vol. 57, pp. 140–150, 1987.

[10] R. D. Gatzke, "The electrode: A measurement systems viewpoint," in *Biomedical Electrode Technology*, A. C. Miller and D. C. Harrison, Eds. London, U.K.: Academic, 1974, pp. 99–116.

[11] H. W. Tam and J. G. Webster, "Minimizing electrode motion artifact by skin abrasion," *IEEE Trans. Biomed. Eng.*, vol. BME-24, pp. 134–139, Mar. 1977.

[12] M. R. Neuman, "Biopotential electrodes," in *Medical Instrumentation, Application and Design*, 2 ed, J. G. Webster, Ed. Boston, MA: Houghton Mifflin, 1992, pp. 227–287.

[13] P. Zipp and H. Ahrens, "A model of bioelectrode motion artifact and reduction of artifact by amplifier input stage design," *J. Biomed. Eng.*, vol. 1, pp. 273–276, 1979.

[14] J. C. Huhta and J. G. Webster, "60-Hz interference in electrocardiography," *IEEE Trans. Biomed. Eng.*, vol. BME-20, pp. 91–101, Mar. 1973.

[15] B. B. Winter and J. G. Webster, "Reduction of interference due to common mode voltage in biopotential amplifiers," *IEEE Trans. Biomed. Eng.*, vol. BME-30, pp. 58–62, Jan. 1983.

[16] ——, "Driven-right-leg circuit design," *IEEE Trans. Biomed. Eng.*, vol. BME-30, pp. 62–66, Jan. 1983.

[17] N. V. Thakor and J. G. Webster, "Ground-free ECG recording with two electrodes," *IEEE Trans. Biomed. Eng.*, vol. BME-27, pp. 699–704, Dec. 1980.

[18] R. Pallas-Areny and J. G. Webster, "Common mode rejection ratio in differential amplifiers," *IEEE Trans. Instrum. Meas.*, vol. 40, pp. 669–676, 1991.

[19] M. J. Burke, "A Microcontroller Based Athletic Cardiotachometer," Ph.D. dissertation, Trinity College, Dublin, Ireland, 1990.

[20] R. Pallas-Areny and J. G. Webster, "Common mode rejection ratio for cascaded differential amplifier stages," *IEEE Trans. Instrum. Meas.*, vol. 40, pp. 677–681, 1991.

[21] D. T. Gleeson, "Low-power ECG Amplifier and Detector," M.Sc. thesis, Trinity College, Dublin, Ireland, 1996.

[22] H. V. Pipberger *et al.*, "AHA Committee Report: Recommendations for standardization of leads and of specifications for instruments in electrocardiography and vectorcardiography," *Circulation*, vol. 52, pp. 11–31, 1975.

[23] J. J. Bailey *et al.*, "AHA Scientific Council Special Report: Recommendations for standardization and specifications in automated electrocardiography," *Circulation*, vol. 81, pp. 730–739, 1990.

[24] L. Brouha, A. Graybiel, and C. W. Heath, "The step test: A simple method of measuring physical fitness for hard muscular work in adult man," *Rev. Can. Biol.*, vol. 2, pp. 86–91, 1943.

Martin J. Burke was born in 1954 in the Republic of Ireland. He graduated from the Institute of Electonic and Radio Engineers (IERE) in 1978 and received the M.Sc. and Ph.D. degrees from Trinity College, Dublin, Republic of Ireland, in 1983 and 1991, respectively.

He is currently a Lecturer in Electronic Engineering in Trinity College. His research interests are in biomedical instrumentation, applications, and related IC design.

Denis T. Gleeson was born in 1964 in the Republic of Ireland. He graduated from the Dublin Institute of Technology, Dublin, Republic of Ireland, in 1991 and received the M.Sc. degree from Trinity College, Dublin, Republic of Ireland, in 1997.

He is currently a Senior Research Engineer with Aritech Irl. Ltd., Dublin, Republic of Ireland, and is working on the development of intelligent security systems.